Modeling of Electro-Mechanical Coupling Problem using the Finite Element Formulation.

Véronique Rochus[a], Daniel Rixen[b], Jean-Claude Golinval[a]

[a]University of Liège, Département d'Aérospatiale, Mécanique et Matériaux, LTAS-Vibrations et Identification des Structures, Chemin des chevreuils, 1, B52/3, B-4000 Liège, Belgium
[b] TU-Delft, Faculty of Design, Engineering and Production Engineering Mechanics - Dynamics, Mekelweg 2, Delft, 2628 CD The Netherlands

ABSTRACT

A modeling procedure is proposed to handle strong electro-mechanical coupling appearing in micro-electro-mechanical systems (MEMS). The finite element method is used to discretize simultaneously the electrostatic and mechanical fields. The formulation is consistently derived from variational principles based on the electro-mechanical free energy. In classical weakly coupled formulations staggered iteration is used between the electrostatic and the mechanical domain. Therefore, in those approaches, linear stiffness is evaluated by finite differences and equilibrium is reached typically by relaxation techniques. The strong coupling formulation presented here allows to derive exact tangent matrices of the electro-mechanical system. Thus it allows to compute non-linear equilibrium positions using Newton-Raphson type of iterations combined with adaptive meshing in case of large displacements. Furthermore, the tangent matrix obtained in the method exposed in this paper greatly simplifies the computation of vibration modes and frequencies of the coupled system around equilibrium configurations. The non-linear variation of frequencies with respect to voltage and stiffness can be then be investigated until pull-in appears. In order to illustrate the effectiveness of the proposed formulation numerical results are shown first for the reference problem of a simple flexible capacitor, then for the model of a micro-bridge.

Keywords: Finite Element Method (FEM), Strong Electro-Mechanical Coupling, Micro-Electro-Mechanical Systems (MEMS), Non-Linearity.

1. INTRODUCTION

When simulating electro-mechanically coupled systems, weak coupling procedures are typically used. The electrostatic field and the mechanical domain are discretized and solved for independently in different analysis steps. Iterations are then performed: the electrostatic solution provides the electrostatic forces on the structure and the structure deformation defines the new boundaries for the electrostatic problem. This method is commonly presented in the literature (see e.g. Lee et al.[1]) and is illustrated in figure 1.

The method proposed here computes the electric and mechanical fields *simultaneously*. Since the problem is non-linear, it must be solved by an iterative algorithm such as the Newton-Raphson method or the Riks-Crisfield's technique.[2] In figure 1 the weak and strong coupling approaches are compared.

The solution strategy proposed in this work consists in the following steps. Given an electric potential applied on the boundaries of the structure, a first solution is obtained by considering the coupled problem linearized around an initial configuration. The resulting structural deformation then defines a modified electric domain and a new linearised problem is defined around the modified configuration and solved for. This process continues until the solution has converged, namely until the electric and mechanical equilibrium are satisfied up to a predefined tolerance (see figure 1). One of the advantages of this formulation is that the tangent stiffness matrix can be explicitly constructed for the coupled problem and therefore, around a given equilibrium configuration, the natural frequency of the electrostatically coupled structure can easily be evaluated.

The following section outlines how the fully coupled finite element approach can be devised by applying a variational approach based on the free energy of the electro-mechanical system. Also we will indicate how the

E-mail: V.rochus@ulg.ac.be, Tel : 32-(0)4- 366 48 52, Fax : 32-(0)4- 366 48 56, http://www.ulg.ac.be/ltas-vis

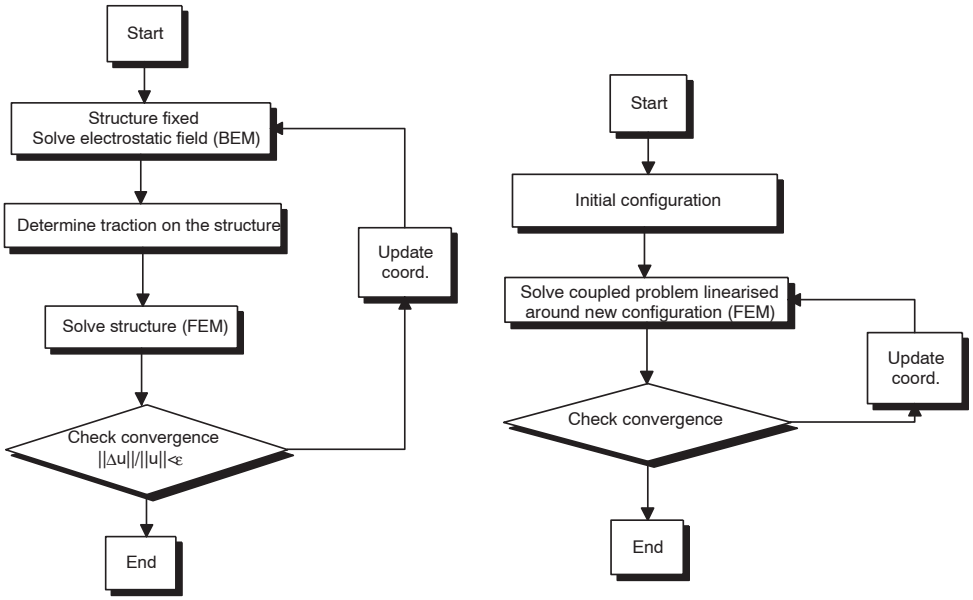

Figure 1. Classical weakly coupled procedure (left) compared to the proposed strongly coupled approach (right).

tangent matrix can be derived and summarize the Newton-Raphson and the Riks-Crisfield method to solve the non-linear coupled problem. The methodology is applied to a simple capacitor problem in section 3 and to a micro-bridge model in section 4. In both cases the obtained results (namely stability limits and eigenfrequency) are compared to analytical solutions.

2. FINITE ELEMENT MODEL

A consistent way of deriving a finite element discretization for the coupled electro-mechanical problem consists in applying the variational principe. Starting from the energy of the coupled system, nodal forces are obtained for an element by derivation of the energy. The tangent stiffness matrix of the coupled problem is then obtained by linearisation of the equilibrium equations in the vicinity of an equilibrium position.

2.1. Total Energy of the coupled system

The total energy of the coupled problem includes the electric and mechanical energies. The expression of energy density results from thermodynamical considerations.[3] Depending on the chosen variables, either the Helmholtz or the Gibbs' free energy have to be used. If intensive variables, namely the mechanical stress $\boldsymbol{T}$ and the electric field $\boldsymbol{E}$, are chosen, Gibbs' energy density has to be considered:

$$G = \frac{1}{2}\boldsymbol{S}^T\boldsymbol{T} - \frac{1}{2}\boldsymbol{D}^T\boldsymbol{E} \tag{1}$$

where $\boldsymbol{T}$ is the stress tensor, $\boldsymbol{S}$ the strain tensor, $\boldsymbol{D}$ the electric displacement tensor and $\boldsymbol{E}$ the electric field. The internal energy on a volume V is then:

$$W_{int} = \int_V \left(\frac{1}{2}\boldsymbol{S}^T\boldsymbol{T} - \frac{1}{2}\boldsymbol{D}^T\boldsymbol{E}\right) dV \tag{2}$$

The constitutive equations determine the relations:

$$\begin{cases} \boldsymbol{T} = \boldsymbol{H}\boldsymbol{S} \\ \boldsymbol{D} = \boldsymbol{\varepsilon}\boldsymbol{E} \end{cases} \tag{3}$$

where $\boldsymbol{H}$ is Hooke's matrix and $\boldsymbol{\varepsilon}$ the permittivity matrix. The compatibility equations are:

$$\begin{cases} S_{ij} = \frac{1}{2}\left(\frac{\partial u_i}{\partial x_j} + \frac{\partial u_j}{\partial x_i}\right) & \text{in } V \\ \boldsymbol{u} = \overline{\boldsymbol{u}} & \text{on } \Gamma_u \end{cases} \qquad \begin{cases} \boldsymbol{E} = -\nabla\phi & \text{in } V \\ \phi = \overline{\phi} & \text{on } \Gamma_\phi \end{cases} \tag{4}$$

where $\boldsymbol{u}$ and ϕ are respectively the mechanical displacement vector and the electric potential, and where ∇ is the gradient operator. These variables will be the unknowns of our problem. The overlined variables $\overline{\boldsymbol{u}}$ and $\overline{\phi}$ are the displacement and potential imposed on the surfaces. The external energy is defined by

$$W_{ext} = \int_V \boldsymbol{u}^T \overline{\boldsymbol{f}}\, dV + \int_{\Gamma_T} \boldsymbol{u}^T \overline{\boldsymbol{t}}\, dS - \int_V \phi\overline{\rho}\, dV + \int_{\Gamma_d} \phi\overline{d}\, dS \tag{5}$$

where $\overline{\boldsymbol{f}}$ is the applied body forces, $\overline{\boldsymbol{t}}$ the surface tractions imposed on Γ_T, $\overline{\rho}$ the imposed charge density and $\overline{d}$ the electric displacement imposed on Γ_d (as shown in figure 2).

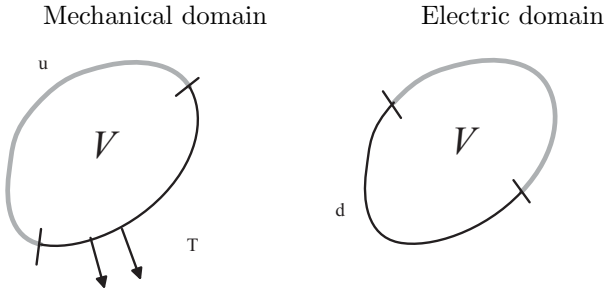

Figure 2. Mechanical and electric domains.

2.2. Internal forces

For sake of conciseness the following developments are outlined for the two dimensional case, but the same reasoning can be used for the three dimensional case. To obtain the internal forces we will use the virtual work principle. Let $\boldsymbol{u}$ be a displacement field and ϕ a potential field verifying the compatibility conditions, implying that these fields are continuous and differentiable. Let $\boldsymbol{u}^*$ be a virtual displacement and ϕ^* a virtual potential such as:

$$\begin{cases} \boldsymbol{u}^* = \boldsymbol{u} + \delta\boldsymbol{u} \\ \phi^* = \phi + \delta\phi \end{cases} \tag{6}$$

The variations satisfying the kinematic constraints. Hence the virtual displacements and potential must be zero on the contour Γ_u and Γ_ϕ where there are imposed, and remain arbitrary on Γ_T and Γ_D where mechanical stress and electric displacements are imposed. The variations δu_i and $\delta\phi$ are then said to be kinematically admissible and the virtual work principle can be applied.

The total energy is stationary for all displacements and potential fields kinematically admissible if and only if the mechanical displacements and electric potential exactly satisfy the equilibrium relations. To find the equilibrium equation of the electromechanical system, we thus must evaluate

$$\delta W_{int} = \delta W_{ext} \tag{7}$$

The internal energy of the coupled problem is:

$$W_{int} = \frac{1}{2}\int_V \boldsymbol{S}^T\boldsymbol{T}\, dV - \frac{1}{2}\int_{V(\boldsymbol{u})} \boldsymbol{D}^T\boldsymbol{E}\, dV = W_m - W_e \tag{8}$$

where W_m is the mechanical energy and W_e the electric one. The integration volume for the electric part depends on the mechanical displacement $\boldsymbol{u}$. The total energy variation due to the displacement yields the mechanical internal forces and its variation with respect to the potential yields the electric equilibrium equation:

$$\left\{ \begin{array}{l} \boldsymbol{f}_m \cdot \delta\boldsymbol{u} = \delta_u W_{int} = \delta_u W_m - \delta_u W_e \\ f_e \;\; \delta\phi = \delta_\phi W_{int} = \delta_\phi W_m - \delta_\phi W_e \end{array} \right. \tag{9}$$

Three of these variations can be evaluated in a straightforward manner. In fact they can be treated as in the standard variational calculus for uncoupled electrostatics and mechanics to obtain

$$\left\{ \begin{array}{l} \delta_u W_m = -\int_V \delta\boldsymbol{u}^T \nabla\boldsymbol{T}\, dV + \int_S \delta\boldsymbol{u}^T \boldsymbol{N}^T \boldsymbol{T}\, dS \\ \delta_\phi W_e = \int_{V(\boldsymbol{u})} \delta\phi^T \, \nabla.\boldsymbol{D}\, dV - \int_S \delta\phi^T \, \boldsymbol{D}.\boldsymbol{n}\, dS \\ \delta_\phi W_m = 0 \end{array} \right. \tag{10}$$

On the other hand, the variation of the electric energy due to the displacement $\boldsymbol{u}$ is not common. In order to express the dependence of the volume of the electric domain with respect to structural displacements let us perform the change of variables

$$\left\{ \begin{array}{l} x = \xi + \delta u_x \\ y = \eta + \delta u_y \\ z = \chi + \delta u_z \end{array} \right. \tag{11}$$

where ξ, η, χ and x, y, z are respectively the coordinates of structural points in the reference configuration and in the perturbed state. The perturbed electric energy is then expressed by

$$W_e^* = \frac{1}{2} \int_V (\nabla\phi)^T \boldsymbol{J}^{-T} \boldsymbol{\varepsilon} \boldsymbol{J}^{-1} (\nabla\phi) \det \boldsymbol{J} dV \tag{12}$$

In this expression, V is now the reference volume $dV = d\xi d\eta d\chi$, ∇ is the gradient with respect to ξ, η, χ and $\boldsymbol{J}$ is the Jacobian of the transformation (11). Recalling that the variations are arbitrarily small, one finds:

$$\boldsymbol{J}^{-1} = \left(\begin{array}{cc} (1 - \delta_\xi u_x) & -\delta_\xi u_y \\ -\delta_\eta u_x & (1 - \delta_\eta u_y) \end{array} \right) \tag{13}$$

where $\delta_\xi u_x$ denotes $\partial \delta u_x / \partial \xi$ and so on.

The internal forces due to the variation of the electric energy with respect to displacements are finally obtained subtracting from the perturbed energy (12) the reference one. After some developments and a dropping of high order terms in δ, its expression can be written as

$$\delta_u W_e = \frac{1}{2} \int_V \boldsymbol{D}^T \left(\begin{array}{cccc} -\frac{\partial\phi}{\partial\xi} & 0 & -2\frac{\partial\phi}{\partial\eta} & \frac{\partial\phi}{\partial\xi} \\ \frac{\partial\phi}{\partial\eta} & -2\frac{\partial\phi}{\partial\xi} & 0 & -\frac{\partial\phi}{\partial\eta} \end{array} \right) \nabla\delta\boldsymbol{u} = \frac{1}{2} \int_V \boldsymbol{D}^T \boldsymbol{F} \nabla\delta\boldsymbol{u} = \boldsymbol{f}_m.\delta\boldsymbol{u} \tag{14}$$

2.3. The tangent stiffness matrix

The stiffness matrix is obtain by linearisation of the internal forces around a equliibrium position:

$$\begin{array}{l} \boldsymbol{f}_m \simeq \boldsymbol{K}_{uu}\boldsymbol{u} + \boldsymbol{K}_{u\phi}\phi \\ \boldsymbol{f}_e \simeq \boldsymbol{K}_{\phi u}\boldsymbol{u} + \boldsymbol{K}_{\phi\phi}\phi \end{array} \tag{15}$$

It is observed that the total coupled matrix is symmetric. The matrix $\boldsymbol{K}_{\phi\phi}$ is the same as the stiffness matrices of the purely electric problem and need not be further discussed. Let us then further discuss the matrix $\boldsymbol{K}_{\boldsymbol{uu}}$ and $\boldsymbol{K}_{\boldsymbol{u}\phi}$.

The coupling matrix $\boldsymbol{K}_{u\phi}$

To evaluate the matrix $\boldsymbol{K}_{u\phi}$, one needs only to derive the second term of the internal mechanical force $\boldsymbol{f}_m$ with respect to the voltage. Performing to that purpose a second variation of (14) no with respect to ϕ, we obtain

$$\delta_\phi \boldsymbol{f}_m \cdot \delta\boldsymbol{u} = \int_V (\nabla\delta\phi)^T \begin{pmatrix} -\varepsilon_{11}\frac{\partial\phi}{\partial\xi} & -\varepsilon_{22}\frac{\partial\phi}{\partial\eta} & -\varepsilon_{11}\frac{\partial\phi}{\partial\eta} & \varepsilon_{11}\frac{\partial\phi}{\partial\xi} \\ \varepsilon_{22}\frac{\partial\phi}{\partial\eta} & -\varepsilon_{22}\frac{\partial\phi}{\partial\xi} & -\varepsilon_{11}\frac{\partial\phi}{\partial\xi} & -\varepsilon_{22}\frac{\partial\phi}{\partial\eta} \end{pmatrix} \nabla\delta\boldsymbol{u} \tag{16}$$

where the matrix in the center of this expression is the coupling matrix $\boldsymbol{K}_{u\phi}$.

The matrix $\boldsymbol{K}_{uu}$

The matrix $\boldsymbol{K}_{uu}$ has two contributions: the first one is due to the stiffness on the domain as in the purely mechanical problem. The second one derives from the dependency of electric force to structural displacements namely

$$\begin{aligned} \delta_u \boldsymbol{f}_m.\delta\boldsymbol{u} &= \int_V \nabla\delta\boldsymbol{u}^T \boldsymbol{H} \nabla\delta\boldsymbol{u}^T \\ &+ \int_V \nabla\delta\boldsymbol{u}^T \begin{pmatrix} D_\xi E_\xi & 0 & D_\xi E_\eta & -\frac{1}{2}(D_\xi E_\xi + D_\eta E_\eta) \\ 0 & \underline{\varepsilon}_{22}(E_\xi)^2 & \frac{1}{2}(D_\xi E_\xi + D_\eta E_\eta) & D_\eta E_\xi \\ D_\xi E_\eta & \frac{1}{2}(D_\xi E_\xi + D_\eta E_\eta) & \underline{\varepsilon}_{11}(E_\eta)^2 & 0 \\ -\frac{1}{2}(D_\xi E_\xi + D_\eta E_\eta) & D_\eta E_\xi & 0 & D_\eta E_\eta \end{pmatrix} \nabla\delta\boldsymbol{u}^T \end{aligned} \tag{17}$$

where the matrix in the center of the expression corresponds to the tangent stiffness matrix. One observes that the electric force introduces an additional stiffness to the mechanical structure.

2.4. Resolution Algorithm

After discretisation, the equilibrium equation resulting from (9) may be written in the matrix form:

$$\begin{pmatrix} \boldsymbol{K}_{uu}(\phi) & \boldsymbol{K}_{u\phi}(\phi) \\ \boldsymbol{K}_{\phi u}(\phi) & \boldsymbol{K}_{\Phi\Phi} \end{pmatrix} \begin{pmatrix} \boldsymbol{U} \\ \boldsymbol{\Phi} \end{pmatrix} = \begin{pmatrix} \boldsymbol{F} \\ \boldsymbol{Q} \end{pmatrix} \tag{18}$$

where $\boldsymbol{Q}$ and $\boldsymbol{F}$ are respectively electric charges and structural forces. This equation constitutes a non-linear coupled system since the matrices are function of the solution ϕ. Equation (18) may be rewritten in terms of the generalised coordinates $\boldsymbol{q}^T = \{\boldsymbol{U}, \boldsymbol{\Phi}\}$:

$$\boldsymbol{r}(\boldsymbol{q}) = \begin{pmatrix} \boldsymbol{K}_{uu}(\boldsymbol{q}) & \boldsymbol{K}_{u\phi}(\boldsymbol{q}) \\ \boldsymbol{K}_{\phi u}(\boldsymbol{q}) & \boldsymbol{K}_{\Phi\Phi} \end{pmatrix} \boldsymbol{q} - \begin{pmatrix} \boldsymbol{F} \\ \boldsymbol{Q} \end{pmatrix} \tag{19}$$

where $\boldsymbol{r}$ is the residual vector. The non-linear system (19) is then solved in an iterative way by means of the Newton-Raphson or Riks-Crisfield methods.[2, 4]

Newton Raphson method

Let us denote $\boldsymbol{q}^k$ an approximate value of $\boldsymbol{q}$ resulting from iteration k. The corrections $\boldsymbol{\Delta q_k}$ are computed by solving the linearised equation

$$\boldsymbol{r}(\boldsymbol{q}^{k+1}) = \boldsymbol{r}(\boldsymbol{q}^k) + \left[\frac{\partial \boldsymbol{r}}{\partial \boldsymbol{q}}\right]_{q^k} \boldsymbol{\Delta q} = 0 \tag{20}$$

where the Jacobian matrix $\boldsymbol{K}^t = \left[\frac{\partial \boldsymbol{r}}{\partial \boldsymbol{q}}\right]_{q^k}$ defines the tangent stiffness matrix. The total displacements are iteratively corrected according to:

$$\boldsymbol{q}_{k+1} = \boldsymbol{q}_k + \Delta\boldsymbol{q}_k \tag{21}$$

until the resulting residual vector comes below a given tolerance.

Riks-Crisfield method

Newton-Raphson method allows to find an equilibrium position solution of the non-linear problem (18) for a given imposed set of structural displacements (or forces) and electric potential (or displacement). However when trying to characterize the quasi-static response of the electromechanical system when for instance the voltage is increased, the Newton-Raphson will not converge if the pull-in potential has been reached since a quasi-static solution no longer exist.

Therefore, in order to follow the quasi-static evolution of the system in terms of applied potential and resulting deformation, one needs to apply a so-called continuation technique. One of these techniques is the Riks-Crisfield method. Calling $\boldsymbol{q}$ the output variables (mechanical displacements and potential) and λ the applied input (imposed potential on electrodes for instance), Riks-Crisfield technique consists in constraining the distance between two computed points in the $\boldsymbol{q}, \lambda$ graph to be at a predefined distance. Hence, instead of prescribing an increment in $\Delta\lambda_i$ from a previous equilibrium computation corresponding to λ_i, a new quasi-static equilibrium is searched for a combined increment in the driving parameter $\lambda_i + \Delta\lambda_k$ and in the system unknown increments such that

$$\boldsymbol{d}_k.\boldsymbol{d}_k = \Delta S_i^2 \tag{22}$$

where $\boldsymbol{d}_k$ locates the position of the point, with respect to the point i and is defined by (see figure 3)

$$\boldsymbol{d}_k = \begin{bmatrix} \Delta\boldsymbol{q}_i + \Delta\boldsymbol{q}_k \\ \Delta\lambda_i - \Delta\lambda_k \end{bmatrix} \tag{23}$$

This equation will be a new constraint to add to the equilibrium equation (20). Thanks to this constraint, the incremental load $\Delta\lambda_i$ becomes an unknown of the problem and will be modified during the process. The Riks-Crisfield method is more complicated than the Newton-Raphson one but permits to pass the maximum point of the analysis curve and to continue the analysis in the unstable region.

(a) Newton-Raphson method

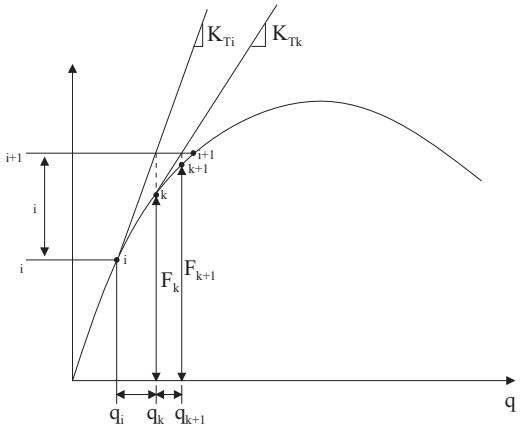

(b) Riks-Crisfield method

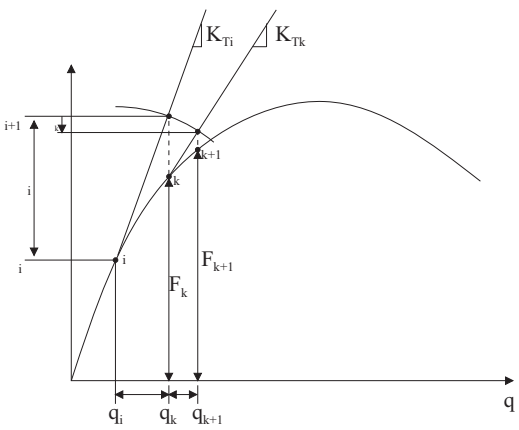

Figure 3. Iterative methods to resolve non-linear problems

3. APPLICATIONS TO A REFERENCE PROBLEM

3.1. Problem

In order to validate the numerical results, the reference problem shown in figure 4 is considered.[5] It consists in a capacitor made of two parallel discs with a voltage applied between them. The upper disc is moveable and is attached to a spring of stiffness k at its centre while the lower disc is fixed. This simplified problem is very representative of the mode of operation of micro-systems such as micro-actuators and micro-accelerometers. A preliminary non-dimensional analysis allows to define what are the assumptions of the problem to be considered.

For this type of problem, the electrostatic assumption is licit.[6] For the sake of simplicity, the electrodes of the capacitor are considered as infinite planes and the electric charges are supposed to be evenly distributed on the surfaces. This approximation allows to neglect fringing fields and to reduce the system to a one-dimensional problem. The voltage is applied between planes '0' and '2' but because of the electrostatic assumption, the system behaves as if the voltage was applied between planes '0' and '1'. The capacitor is in vacuum and no damping is considered in the model. Only the strong coupling between the electric and the mechanical fields will be studied.

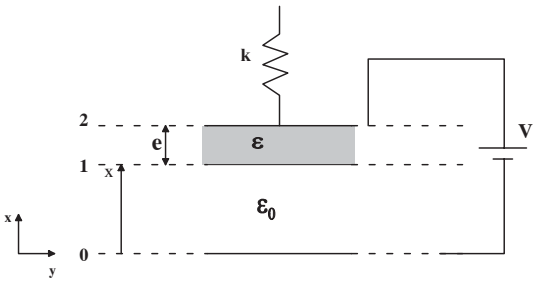

Figure 4. Definition of a reference problem

3.2. Analytical Solution

Dynamic equilibrium equation

The dynamic equilibrium equation of the capacitor is written under the assumption of rigid plates. In this assembly, two mechanical forces occur. First, when the plate moves down from its rest position x_0, an upward force is created :

$$\boldsymbol{f}_m = -k(x - x_0)\boldsymbol{e}_x \tag{24}$$

where k is the stiffness of the spring per unit area. The second mechanical force to be considered is the force due to gravity :

$$\boldsymbol{f} = m\boldsymbol{g} \tag{25}$$

where m is the surface mass density of the plate. Because of the small size of the structure, the gravitational force is very small compared to the electric and the spring restoring forces, and may be neglected. For the electric part, the only known imposed value is the voltage V between the planes '0' and '2'. The electric force on the plate surface is then determined by[7] :

$$f_e = -\frac{1}{2}\epsilon_0 \frac{V^2}{x^2} \tag{26}$$

where ϵ_0 is the permittivity of the electric domain between the electrodes. This result can also be obtained by energy considerations in the capacitor. Writing Newton's second law for the capacitor system, we obtain :

$$m\ddot{x} = -k(x - x_0) - \frac{1}{2}\epsilon_0 \frac{V^2}{x^2} \tag{27}$$

Stability analysis

It can be noted from equation (27) that the dynamic behaviour of the structure depends on the applied voltage V, the spring stiffness k and its rest position x_0. A coupling term arises since the presence of the electric field adds a non-linear term in the equation of motion. The electric force applied to the surface induces an additional stiffness that modifies the natural frequency of the mechanical system. In the following, the influence of parameters V and k is discussed for a given value of x_0 equal to 1 μm. The solutions of the system corresponding to different initial conditions are shown in the phase diagrams of figure 5. When no voltage is applied to the capacitor, the system is stable as shown in figure 5(a). When a voltage is applied, an instability zone occurs around the stability zone (figure 5(b),(c)). When the plates come closer, the electric force may

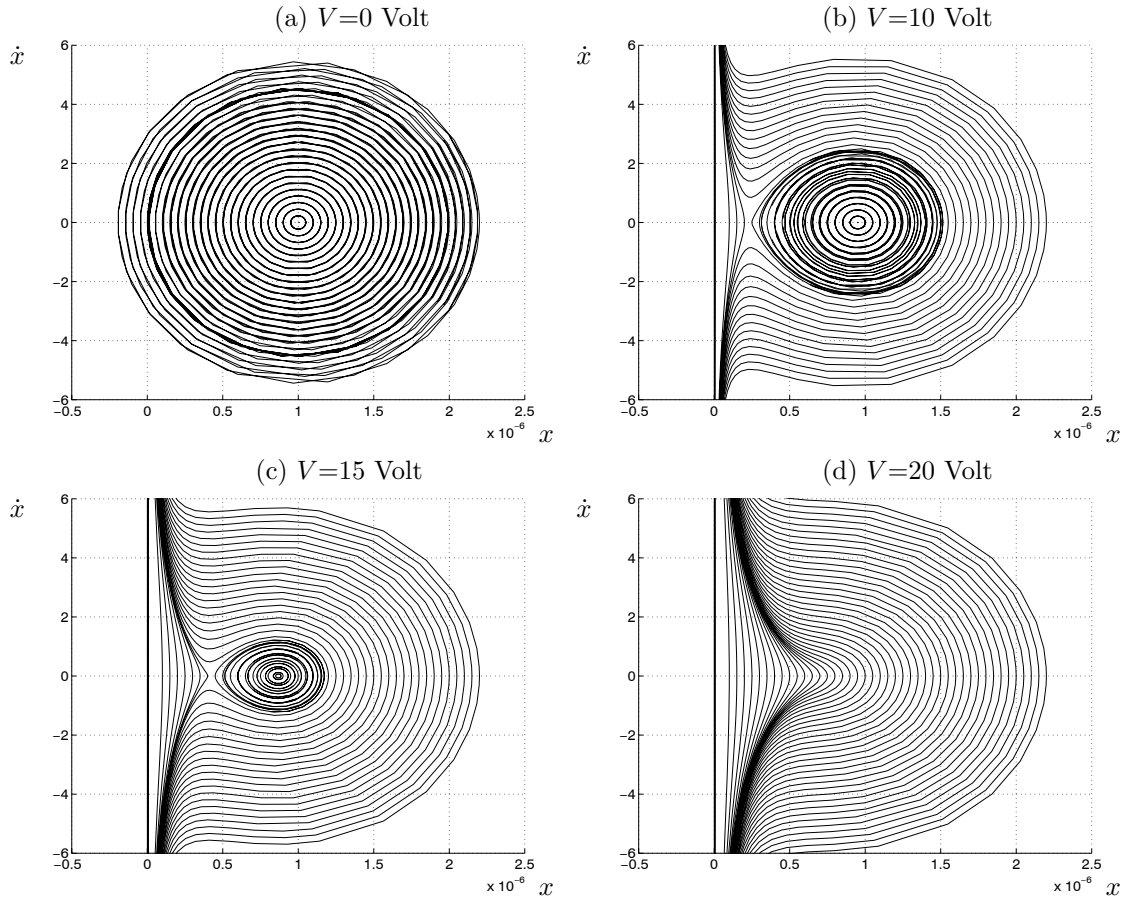

Figure 5. Phase diagrams for increasing values of the applied voltage.

become higher than the spring restoring force and the plates stick together. As voltage increases, the stable zone reduces and vanishes when the ratio $\frac{V^2}{k}$ exceeds a given threshold value equal to 0.33×10^{-7} in this example.

Natural frequency shifting

To calculate the natural frequency of the structure, the system must be linearised around its dynamic equilibrium position noted x_e. It results that the natural frequency ω_0 of the system is a function of the applied voltage :

$$\omega_0 = \sqrt{\frac{(k - \epsilon_0 \frac{V^2}{x_e^3})}{m}} \tag{28}$$

Note that the natural frequency $\sqrt{k/m}$ of the pure mechanical system is retrieved if the electric field is equal to zero. Equation (28) shows that an increase of the voltage causes a decrease of the natural frequency of the system. When the pull-in voltage in reached the eigenfrequency becomes null.

3.3. Finite Element Calculations

To illustrate the influence of the coupling between the mechanical and electric fields, we consider the one-dimension model shown in figure 6 in which the capacitive system is made of three electric elements and three mechanical elements. The mechanical nodes are noted x_i and the electric nodes ϕ_i (i=1,...4). The boundary conditions are:

$$x_4 = 0, \quad \phi_1 = 0, \quad \phi_4 = V \tag{29}$$

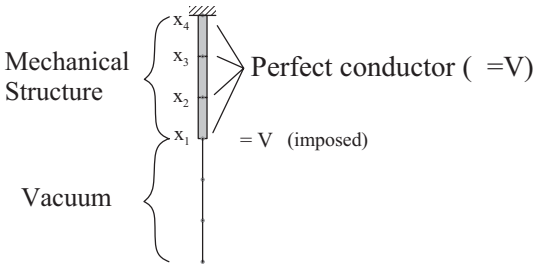

Figure 6. One-dimension problem

The tangent matrix corresponding to the free degrees-of-freedom of this problem takes the form :

$$\left(\begin{array}{cc|ccc} -5.3124\,10^{-5} & 2.6562\,10^{-5} & 0 & 0 & 0 \\ 2.6562\,10^{-5} & -5.3124\,10^{-5} & \mathbf{-265.62} & 0 & 0 \\ \hline 0 & \mathbf{-265.62} & \mathbf{1.29919\,10^{12}} & -1.30185\,10^{12} & 0 \\ 0 & 0 & -1.30185\,10^{12} & 2.6037\,10^{12} & -1.30185\,10^{12} \\ 0 & 0 & 0 & -1.30185\,10^{12} & 2.6037\,10^{12} \end{array}\right) \left(\begin{array}{c} \phi_2 \\ \phi_3 \\ \hline x_1 \\ x_2 \\ x_3 \end{array}\right) \tag{30}$$

The first two lines of this matrix correspond to the electric nodes and the other ones to the mechanical nodes. It can be observed that coupling terms appear between the mechanical and the electric degrees-of-freedom. It also follows that the stiffness of the structure decreases as voltage increases. The equilibrium position of the system is then computed using the Newton-Raphson procedure described earlier. A modification of the static equilibrium position is observed when a voltage is applied as shown in figure 7(a). It is also found that the natural frequency of the structure decreases when voltage increases as shown in figure 7(b). The numerical results are consistent with the analytical developments: in figures 7(a) and (b), the numerical results (black points) are compared to the analytical values (solid line) for both the equilibrium position and the natural frequency. The perfect agreement between these results allows to validate the numerical approach.

(a) Equilibrium position

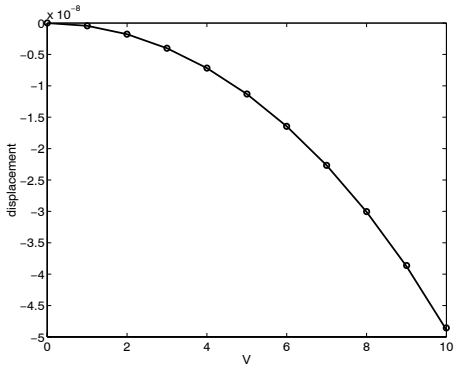

(b) Natural frequency shifting

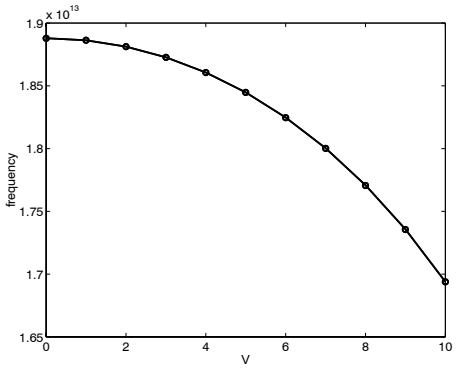

Figure 7. Equilibrium position and natural frequency function of the applied voltage for a spring stiffness of 10^{10} N/m.

4. APPLICATION TO A MICRO-BRIDGE

4.1. Problem Definition

We will now study the behaviour of a beam type resonator presented by Lee et al.[1] The resonator is composed of two electrodes: a clamped-clamped beam and a substrate as shown in figure 8. The beam is made out of silicion. Its density and its Young modulus are respectively of 2330 kg/m^3 and 130GPa. The natural frequencies of the structure will be evaluated as well as its pull-in voltage.

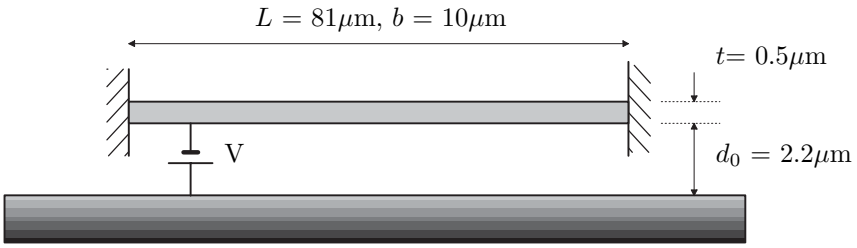

Figure 8. Micro-bridge.

4.2. Analytical Solutions

The beam structure is a little bit more complicated than in the one dimensional problem. No analytical solution can be found. In fact, beam bending and non-uniform load repartition have to be taken into account. To check out numerical results, we will use the analytical approximations proposed by Pamidighantam et al.[8] and by Roark.[9]

First, we will study the evolution of the natural frequency when the voltage increases. The natural frequency of a structure without an applied tension is:

$$f = \frac{(4.730)^2 t}{2\pi\sqrt{12}L^2}\sqrt{\frac{E}{\rho}} \tag{31}$$

where the material properties are taken into account with ρ the mass density and E the Young modulus. The thickness of the beam is denoted by t and its length by L. The frequency shifting will be compared with numerical results obtained by Lee et al..[1]

Another interesting quantity is the pull-in voltage. When the pull-in voltage is applied, the plates stick together. To estimate the pull-in voltage, we use the approximate expression proposed by Pamidighantam et al.[8]:

$$V_{PI} = \sqrt{\frac{8K_{eff}d_0}{27\varepsilon_0 A_{eff}}} \tag{32}$$

where K_{eff} is the effective stiffness of the beam, A_{eff} its effective area, d_0 the initial gap and ε_0 the permittivity. The effective stiffness includes the contribution of the bending stiffness of the beam, the axial tension and the non-linear stiffening due to large displacements. In our case, only the bending stiffness has to be taken into account. The stiffness reduces to

$$K_{eff} = \frac{32Ebt^3}{L^3} \tag{33}$$

The effective area accounts for two effects: the variation of the gap spacing along the beam and the fringing field effects along the edge of the beam. In the case of a fixed-fixed beam large enough to neglect the fringing field, the area A_{eff} is:

$$A_{eff} = 0.6bL \tag{34}$$

4.3. Finite Element Results

The resonator is represented by a two dimensional problem. We use a Riks-Crisfield algorithm to pass the maximum and thereby to accurately evaluate the pull-in voltage.

Pull-in voltage

The pull-in voltage evaluated by the analytical formula is 74.5V. In figure 9 is plotted the graph of displacement when the applied voltage changes. The displacement first increases when the applied voltage increases until the pull-in voltage is reached. Then we enter in the instable area of the curve. Physically the plates stick together. Thanks to our approach we can plot the curve beyond this critical value and enter the unstable area as if the applied voltage was reduced while the displacement increases so that equilibrium can be maintained.

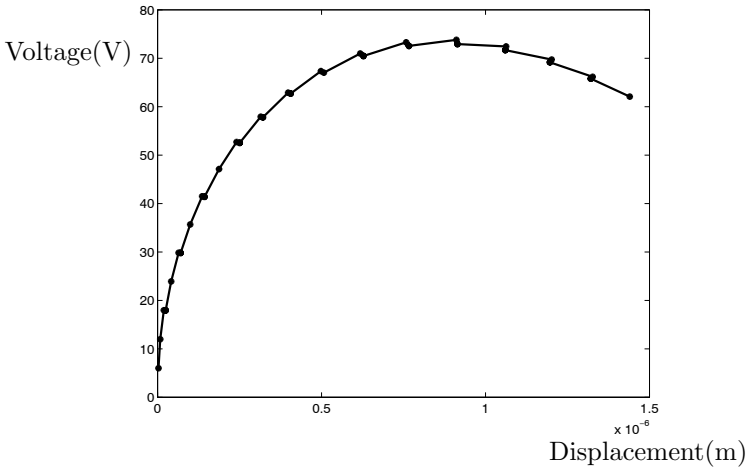

Figure 9. Micro-bridge: displacement as function of tension applied between the electrodes

Frequency shifting

In the present case, the natural frequency without applied tension calculated by relation (31) is 585 kHz. Lee et al.[1] found a frequency of 620 kHz. With our modeling, we found 593 kHz. The type of elements used to simulate the structure influences its stiffness. In this case, they overestimate the stiffness of the structure and thus the frequency is slightly higher than the analytical one. Figure 10 shows that the decrease due to applied voltage is the same for both methods. To estimate the natural frequency, Lee et al. calculate the eigenmodes of the pure mechanical structure and project the equilibrium equations of the coupled problem on these eigenmodes. After a perturbation analysis to find the linearized stiffness, they obtain the natural frequency of the coupled problem. Note that such a method is accurate only when the electric force does not significantly influence the eigenmodes of the coupled structure. The frequency is calculated up to the pull-in. For larger voltages, the plates stick together and the natural frequency is not defined any more.

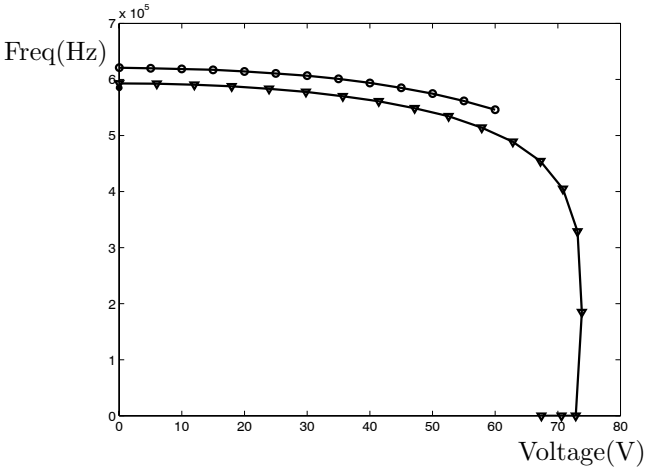

Figure 10. Frequency shifting when a voltage is applied between the electrodes. Lee's results are indicated by circles and our results are indicated by triangles.

5. CONCLUSION

Unlike usual methods which iterate between a mechanical and an electric solvers, the method proposed in this paper consists in resolving the mechanical and electric equilibrium equations at the same time. The formulation is based on the total energy of the coupled problem. The electric force appears naturally in the mechanical and

electric equilibrium equations. After linearization of the equations, the tangent stiffness matrix is computed. This matrix allows us to use nonlinear resolution algorithms such as the Newton-Raphson and the Riks-Crisfield ones. Also, computing eigenfrequencies around a equilibrium position is straightforward.

This new formulation was first validated in a simple one-dimensional case. The analytical expression of the displacement as a function of the applied voltage and of the eigenfrequency shifting allowed us to check our results precisely. The validation then pursued with a more complex case: a clamped-clamped beam representing a micro-bridge. The Riks-Crisfield algorithm permits a precise evaluation of the pull-in voltage. The first eigenfrequency has been computed and compared to results published elsewhere.

ACKNOWLEDGMENTS

The authors would like to thank I. Klapka (Open Engineering, Belgium) and Dr. P. Dular (University of Liège, Belgium) for there valuable support and constructive comments. The first author acknowledges the financial support of the Belgian National Fund for Scientific Research. The second author acknowledges the financial support of the Koiter Institute form the Delft University of Technology, The Netherlands.

REFERENCES

1. W. Lee, K. Kwon, B. Kim, J. Cho, and S. Young, "Frequency-shifting analysis of electrostatically tunable micro-mechanical actuator," *Journal of Modeling and Simulation of Microsystems,* **Vol.2, No.1**, pp. 83–88, 2001.
2. M. Crisfield, *Non–Linear Finite Element Analysis of Solids and Structures*, John Wiley, 1991.
3. T. Ikeda, *Fundamentals of piezoelectricity*, OXFORD, 1996.
4. J. Warren, *Nonlinear Stability Analysis of Frame-Type Structures with Random Geometric Imperfections using a Total-Lagrangian Finite Element Formulation*, 1997.
5. V.Rochus, P.Duysinx, and J. Golinval, "Finite element analysis of the electro-mechanical coupling in mems," *ACOMEN 2002, Second international conference on advanced computational method in engineering* , 2002.
6. P. Hammond, *Electromagnetism for Engineers*, Pergamon, 1986.
7. E. Duran, *Electrostatique*, Masson et Cie, 1964.
8. S. Pamidighantam, R. Puers, and H. A. C. Tilmans, "Pull-in voltage analysis of fixed-fixed beams," *proc. MME2001* , pp. 269–272, 2001.
9. W. C. Young, *Roark's Formulas for Stress and Strain*, Mc. Graw-Hill, 1989.